Earthquake Engineering & Structural Dynamics
The Journal of the International Association for Earthquake Engineering

EARTHQUAKE ENGINEERING & STRUCTURAL DYNAMICS
Earthquake Engng Struct. Dyn. 2012; **41**:1693–1707
Published online 17 January 2012 in Wiley Online Library (wileyonlinelibrary.com). DOI: 10.1002/eqe.1198

A procedure on ground motion selection and scaling for nonlinear response of simple structural systems

Bekir Özer Ay and Sinan Akkar*†

Earthquake Engineering Research Center, Middle East Technical University, 06800 Ankara, Turkey

SUMMARY

This study presents a ground-motion selection and scaling methodology that preserves the basic seismological features of the scaled records with reduced scatter in the nonlinear structural response. The methodology modifies each strong-motion recording with known fundamental seismological parameters using the estimations of ground-motion prediction equations for a given target hazard level. It provides robust estimations on target building response through scaled ground motions and calculates the dispersion about this target. This alternative procedure is not only useful for record scaling and selection but, upon its further refinement, can also be advantageous for the probabilistic methods that assess the engineering demand parameters for a given target hazard level. Case studies that compare the performance of the proposed procedure with some other record selection and scaling methods suggest its usefulness for building performance assessment and loss models.

Received 30 May 2011; Revised 24 September 2011; Accepted 30 October 2011

KEY WORDS: record selection and scaling; linear and nonlinear structural response; ground-motion variability; seismic risk assessment

1. INTRODUCTION

Selection and scaling of accelerograms is a frequently applied tool among practicing engineers to assess the structural performance for a given target hazard level. From the objective point of view most of the ground-motion selection and scaling methodologies aim either to give an accurate estimation of median structural response or to predict the full probability distribution of response for a given scenario event. The earthquake scenario is generally described for a ground-motion intensity level associated with a magnitude and distance pair.

Studies on the selection and scaling procedures date back to the mid-1980s. In their study, Nau and Hall [1] concluded that record scaling with respect to spectral ordinates reduce the dispersion on the structural response. Later, Martinez-Rueda [2] and Kappos and Kyriakakis [3] investigated scaling methodologies that directly depend on the structural response. The study conducted by Shome *et al.* [4] indicated that scaling of recordings by considering the median spectral ordinate of the ground-motion bin at the fundamental period would result in lesser dispersion in the structural response. Bommer and Acevedo [5] pointed to the importance of magnitude agreement between the target earthquake scenario and selected recordings. Naeim *et al.* [6] emphasized that not only the magnitude but also a proper distance interval that matches the target hazard scenario is advantageous while selecting the ground motions. In their paper, Cimellaro *et al.* [7] observed that the magnitude and distance properties of the selected ground motions affect the dispersion on the damage indices. Watson-Lamprey and

*Correspondence to: Sinan Akkar, Earthquake Engineering Research Center, Middle East Technical University, 06800 Ankara, Turkey.
†E-mail: sakkar@metu.edu.tr

Abrahamson [8] highlighted the shortcomings of excessive scaling that may invoke the bias in the structural response. Controversially, other studies (e.g., Ref. [9]) advocated that large amounts of scaling would not produce biased nonlinear structural response unless the spectral shapes of the chosen recordings follow trends significantly different than the target. One of the ground breaking methodologies (conditional mean spectrum, CMS) on the selection and scaling of recordings has been proposed recently by Baker [10] whose initial phases were presented in the collaborative studies of Baker and Cornell [11, 12]. The CMS provides the expected response spectrum conditioned on the occurrence of a target spectral ordinate associated with a magnitude and distance pair and can be used efficiently for selecting scenario-specific ground motions.

Haselton [13] has recently classified the above methodologies (and many others) into five major groups according to their fundamental features. Almost all methods in these groups primarily intend to obtain recordings with magnitude and distance properties closely matching the scenario event of interest. However, each group differs in several points as they impose numerous constraints on the proposed selection and scaling approach to obtain an optimum suite of recordings that comply with the objectives described in the first paragraph. Methods in the first group simply scale each ground motion to a target spectral level after selecting the recordings having similar magnitude and distance ranges of the scenario earthquake. The method proposed by Shome *et al*. [4] is the benchmark study for the procedures in this group. Although the essential component in [4] is to have zero dispersion of scaled recordings about the target spectral level, it also approximates the probability distribution of the structural response subjected to the scaled recordings. Its simplicity and the practicality of the used concepts are the advantages of this procedure. Nonetheless, various studies (e.g., Ref. [14]) have shown that this method can result in significant dispersion about the median structural response as the level of nonlinearity increases. The second group of methods are the code procedures (e.g., Refs. [15–17]) and use appropriate scaling factors over a range of periods such that the average value of response spectra of the scaled recordings closely follow the target design spectrum. Recordings scaled by these methods may lead to conservative median structural response for severe earthquake scenarios because scaling is commonly conducted over a wide range of spectral periods using the uniform hazard spectrum that is associated with large spectral ordinates [10]. The third group of methods use the CMS concept of Baker [10] for selecting the ground motions. This method uses simple amplitude scaling of ground motions over a period range and aims at obtaining reliable estimations of the median structural response without describing the probability distribution of structural response at the target hazard level. The selection and scaling methods in the fourth group consider the epsilon at the fundamental period of the structure that is obtained from the deaggregation of a site-specific probabilistic hazard analysis (e.g., [11]). They use the epsilon as a proxy for the spectral shape and select ground motions with epsilon values that closely match the epsilon value determined from deaggregation. These methods are easy to implement because they only try to match the epsilon instead of matching a range of spectral ordinates in selection and scaling. However, they may result in variations in the median structural response among different sets of ground motions assembled for the same hazard level [13]. Different than the above four groups, the methods in the fifth group consider a close match between inelastic spectral ordinates of the target scenario and selected ground motions. These methods consider the factors important to nonlinear structural response that may result in optimum selection and scaling of recordings to render a better assessment of inelastic structural behavior. However, if the target scenario is based on elastic spectral ordinates, common in many seismic hazard studies, these methods require realistic estimations of inelastic target. Therefore, the accuracy of these methods is limited to the performance of the tools used to relate elastic and inelastic spectral ordinates in such cases.

Our major objective in this paper is to introduce a record selection and scaling strategy to be used in the performance assessment of nonlinear structural systems for a given scenario event. Given a relatively larger ground-motion dataset, the method considers the differences between the individual recordings and their estimations from a ground-motion predictive model. This information is then used to select and scale the optimum subset of ground motions whose median spectral ordinate matches the target hazard level. The optimum recording set has the least dispersion about this target considering that the major concern is the accurate estimation of the median structural response. The method can precisely calculate the dispersion about the median structural response when the structure behaves in the elastic range whereas it can provide a good estimation of this uncertainty

DOI: 10.1002/eqe

for systems responding in the post-elastic range. In essence our method preserves the inherent aleatory variability in the selected recordings without manipulating their inherent features excessively. Moreover, it is capable of describing the uncertainty about median structural response either in the elastic or inelastic range for a given elastic target hazard. This feature makes it as a useful tool for the current site-specific hazard studies. The paper first introduces the proposed approach and then tests its limitations by comparing its performance with alternative methodologies in the literature.

2. SELECTION AND SCALING METHODOLOGY FOR LINEAR SYSTEMS

The proposed methodology does the final selection of ground motions by estimating the dispersion (standard deviation about the target intensity) of alternative ground-motion bins assembled from a larger dataset. In the subsequent sections we first introduce the selection method that is followed by the scaling procedure. We note that the proposed selection and scaling methodology has a nested structure. This section introduces the approach for linear structural systems that is extended for nonlinear structural behavior in the latter parts of the text.

2.1. Selection of ground-motion records

The number of recordings to be used in the evaluation of structures is a critical issue as it may depend on the complexity and functionality of the structural system. Various studies proposed alternative methods to select n accelerograms from a ground-motion dataset of k recordings (e.g., Refs. [7, 9, 10, 12, 18, 19]). For example Cimellaro *et al*. [7] suggest using at least 20 accelerograms to have an accurate estimation on the fragility functions of a first-mode dominant nondegrading building if the ground-motion intensity is chosen as spectral acceleration in the analysis. They also indicate that the minimum number of scaled recordings should be 10 for estimating the first-story drift response with an error less than 10%. In their study, Hancock *et al*. [19] concluded that three recordings that are scaled to the elastic spectral acceleration at the fundamental period are required to predict the peak roof drift of an 8-story regular wall-frame reinforced concrete (RC) building within $\pm 10\%$ accuracy with a confidence level of 64%. Notwithstanding, the common code approach (e.g., Refs. [15–17, 20]) requires a minimum number of seven accelerograms for the median estimation of structural response with limited error. More recently, a report published by the Applied Technology Council; ATC-58 [21] suggests using at least 11 accelerograms for estimating the full probability distribution of building response under a specific scenario event. The general consensus in all these cited references is to select the ground motions from a magnitude range in the vicinity of target scenario magnitude. This common point is quantified as 0.20 magnitude units at either side of the target magnitude [5] that is similar to Stewart *et al*. [22] who suggested the magnitude interval to be ± 0.25 units about the target magnitude (M_{target}). The sensitivity of dynamic structural response to source-to-site distance is found to be less prominent by these studies (i.e., Refs. [5, 22]).

Following the above cited references, we implemented the below criteria while assembling the ground-motion dataset of k candidate accelerograms:

1. $M_{\text{target}} - 0.25M \leqslant M_{\text{target}} \leqslant M_{\text{target}} + 0.25M$,
2. $d_{\text{target}} - 25\,\text{km} < d_{\text{target}} < d_{\text{target}} + 25\,\text{km}$,
3. Recordings of same style-of-faulting and site class as imposed by the target hazard scenario.
4. If the number of recordings that comply with the third criteria is not sufficient to assemble the dataset of candidate accelerograms, relax them. However, accelerograms showing fairly similar site features should be considered even if the site class constraint is relaxed (e.g., National Earthquake Hazards Reduction Program, NEHRP C and D soil classes for a site located in NEHRP C soil class or vice versa — see BSSC [23] for NEHRP soil classifications).

Strictly speaking, the style-of-faulting and soil conditions influence the ground-motion behavior and its amplitude. Consequently, accelerograms failing to meet the specific fault mechanism and soil conditions imposed by the target scenario would increase the bias in the structural response. On the other hand, we had to relax the rules on these two parameters to have a fair amount of candidate accelerograms to be used in the ground-motion selection procedure. Nevertheless, the proposed

DOI: 10.1002/eqe

procedure still acknowledges the actual style-of-faulting and site class features of each candidate accelerogram during its implementation as discussed in the following section. The number of bins, $C(k,n)$, containing n accelerograms assembled from the ground-motion dataset of k recordings is given in Equation (1).

$$C(k,n) = \binom{k}{n} = \frac{k!}{n!(k-n)!} \quad 0 \leqslant n \leqslant k \tag{1}$$

The total number of accelerograms (n) in each bin is set to 10, which is a compromise among the suggestions proposed in the referred literature. In other words, among the k candidate accelerograms, the procedure selects and scales 10 optimum recordings that result in the least dispersion about the target hazard level. Given $n = 10$, we constrained the number of candidate accelerograms (k) in the ground-motion dataset to 20 because our studies showed that the computational burden and reduction of dispersion about the target hazard level are optimized with this choice. For a ground-motion dataset of 20 candidate accelerograms, the total time of running the entire methodology is approximately 90 s on an ordinary PC, which is approximately 10 times less if k is taken as 22. The dispersion of the optimum recording set becomes stable both for linear and nonlinear cases when the ground-motion dataset of candidate recordings constitutes 20 recordings. The population of ground-motion recordings in each alternative bin can be established by using a mathematical software such as MATLAB [24].

The methodology described for the identification of optimum recording set can be considered as a computational burden without any merits. However, the computation of standard deviation for each alternative bin is carried out by a theoretical expression presented in the next section that significantly speeds up this process. Moreover, because the selection and scaling are conducted consecutively, the optimum recording set will be delivered as scaled at the end of the entire procedure.

2.2. *Scaling methodology*

The proposed scaling methodology constrains the scaling to the difference between the actual ground motion and its estimation from a representative ground-motion prediction equation (GMPE). This is similar to the epsilon (ε) concept introduced by Baker and Cornell [11, 12] in ground motion scaling. Given a suite of ground motions, each record is scaled to its individual target intensity instead of scaling all records to a common target intensity level (e.g., Ref. [4]). Scaling all records to common target intensity may artificially suppress the variability in the ground motion that contradicts the inherent nature of earthquake mechanism. Such a procedure may also yield an incomplete vision about the likely amplitudes of future ground motions of similar nature.

The methodology linearly modifies the records in terms of spectral ordinates and peak ground motion values. In the following lines we will describe the procedure for a spectral ordinate because of its frequent use among engineers. We will use spectral displacement (S_d) because the later parts of the text describe the nonlinear extension of the procedure using the nonlinear peak displacements of SDOF systems that are of particular interest for assessing the performance of structures under the scenario event. Nonetheless, the proposed procedure is equally applicable to pseudo-spectral acceleration (PS_a) and peak ground motion values (e.g., peak ground acceleration and velocity; PGA and PGV, respectively).

Given the target spectral displacement at a specific period ($\bar{S}_{\text{dtarget}}(T)$) that is obtained from a deterministic or probabilistic site-specific hazard analysis, the procedure scales the spectral displacement of each record i ($S_{d,i}(T)$) to its individual target level ($S_{\text{dtarget},i}(T)$). To fulfill this objective, we define two important parameters. The first parameter is the logarithmic difference ($\varepsilon\sigma_{\text{Sdi}}$) between the spectral displacement of the record, $S_{d,i}(T)$, and the corresponding median ground motion estimation obtained from the selected GMPE ($\bar{S}_{d,i}(T)$). Equation (2) presents the computation of $\varepsilon\sigma_{\text{Sdi}}$.

$$\varepsilon\sigma_{\text{Sdi}} = \ln\left(S_{d,i}\right) - \ln\left(\bar{S}_{d,i}\right) \tag{2}$$

We account for the actual style-of-faulting and site class information of the recordings in the computation of $\bar{S}_{d,i}(T)$ to partially balance the relaxed criteria on these seismological parameters

DOI: 10.1002/eqe

during the selection of candidate accelerograms. The second parameter is the so called scaling origin, θ, a reference spectral value that is used to have an exact match between the target spectral displacement ($\bar{S}_{\text{dtarget}}(T)$) and the mean of the spectral ordinates of the selected ground motions. For n recordings in a ground-motion bin, the scaling origin θ has the following general form:

$$\theta = \ln\left(\bar{S}_{\text{dtarget}}\right) - \ln\left(\frac{\sum_{i=1}^{n} \exp(\varepsilon\sigma_{\text{Sdi}})}{n}\right) \tag{3}$$

After determining θ for a set of n recordings, $S_{\text{dtarget},\,i}$ is computed by modifying the individual $S_{\text{d},\,i}$ of each accelerogram by a linear scaling factor, γ_i, that is given in Equation (4).

$$\gamma_i = \frac{S_{\text{dtarget},i}(T)}{S_{\text{d},i}(T)} = \frac{\exp(\theta + \varepsilon\sigma_{\text{Sdi}})}{S_{\text{d},i}(T)} \tag{4}$$

Equation (4) defines the linear scaling factor γ_i for each record in terms of θ and $\varepsilon\sigma_{\text{Sdi}}$. The numerator term, $S_{\text{dtarget},\,i}(T)$, is a linear function of θ and $\varepsilon\sigma_{\text{Sdi}}$ in logarithmic scale. γ_i should be applied either to one or both horizontal components of the accelerogram to maintain the consistency between scaling and horizontal component definition of the GMPE. The major assumption in Equation (4) is the independence of σ between the target event and the record-specific event. The entire concept is illustrated in Figure 1.

The average of $S_{\text{dtarget},\,i}$ values for a given bin will yield the target hazard, $\bar{S}_{\text{dtarget}}$. Note that the above scaling preserves the inherent record-to-record (aleatory) variability. We believe that this is a more viable way of representing actual ground-motion features rather than scaling the subject records directly to a common target intensity level. This approach, in a way, is similar to the scaling methodology followed by Buratti *et al.* [25]. The major difference between the methodology presented in this article and Buratti *et al.* [25] is that the latter is devised for estimating the full probabilistic distribution of the structural response by making use of the correlation between the building drift and spectral acceleration. Our methodology brings forward the better estimation of the median structural behavior as indicated in Section 1.

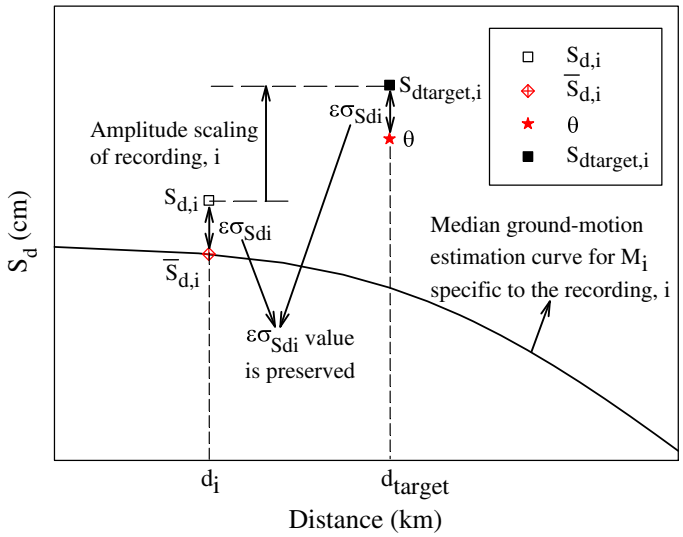

Figure 1. Scaling of ith record with known seismological parameters (M_i, magnitude, site class, style-of-faulting etc.) to its individual target intensity level according to the proposed procedure.

DOI: 10.1002/eqe

The information revealed from this procedure can also serve to define the distribution of scaled ground motions about $\bar{S}_{\text{dtarget}}(T)$. Assuming log-normal distribution for spectral response, one can calculate the expected value ($\lambda_{S_{\text{dtarget}}}$) and standard deviation ($\zeta_{S_{\text{dtarget}}}$) of the scaled ground motions.

$$\lambda_{S_{\text{dtarget}}} = \theta + \frac{\sum_{i=1}^{n} \varepsilon\sigma_{\text{Sdi}}}{n} = \theta + \mu_{\varepsilon\sigma} \tag{5}$$

$$\zeta_{S_{\text{dtarget}}} = \sqrt{\frac{1}{n-1} \cdot \sum_{i=1}^{n} \left(\varepsilon\sigma_{\text{Sdi}} - \mu_{\varepsilon\sigma}\right)^2} \tag{6}$$

The standard deviation, $\zeta_{S_{\text{dtarget}}}$, is the dispersion measure used in the selection procedure. Thus, for each candidate bin, scaling and computation of $\zeta_{S_{\text{dtarget}}}$ is conducted simultaneously. Among the alternative bin combinations, the one yielding the least dispersion about the target hazard level (i.e, $\left(\zeta_{S_{\text{dtarget}}}\right)_{\min}$) is the optimum recording set to be used in the verification of the structure under consideration.

The overall procedure is illustrated using a target scenario determined from the probabilistic seismic hazard analysis conducted for a fictitious building located on a firm soil (NEHRP C). The fundamental period (T_1) of the building is 0.3 s. (The target scenario and fictitious building will be used throughout the text to illustrate the concepts introduced in this study). The fault source of 200 km length that is likely to produce the damaging future earthquakes in the area of interest is assumed to have a strike–slip mechanism. For a return period of 475 years the deaggregation of hazard yielded $M_{\text{target}} = 7.15$ (in terms of moment magnitude, M_w) and $d_{\text{target}} = 22.5$ km (in terms of Joyner-Boore distance, R_{JB}) with an epsilon value of 1.44. The corresponding target spectral displacement (i.e., $\bar{S}_{\text{dtarget}}(T)$) is 2.06 cm, which is computed from the Akkar and Bommer [26] ground-motion predictive model that is consistent with the seismotectonic settings of the fictitious case study. Following the criteria introduced in the previous section, we first assembled a ground-motion dataset of 20 candidate accelerograms. After determining the alternative recording sets of 10 accelerograms, the proposed procedure identified the optimum recording set that yields a minimum standard deviation of $\left(\zeta_{S_{\text{dtarget}}}\right)_{\min} = 0.111$ among those ranging up to 0.651. Table I lists the 20 candidate accelerograms with their seismological properties and spectral values used in the calculations. The ground motions identified in the optimum recording dataset are listed in bold letters together with their scaling factors, γ_i, which are computed in terms of $\varepsilon\sigma_{\text{Sdi}}$. The average of scaled individual target spectral ordinates ($S_{\text{dtarget},\,i} = \gamma_i S_{\text{d},\,i}$) yields the target spectral ordinate ($\bar{S}_{\text{dtarget}}$).

Figure 2 shows some of the specific features of the scaling procedure. The left panel presents the linear variation of scaled spectral displacements (i.e., $\ln(S_{\text{dtarget},\,i}(T))$ as a function of $\varepsilon\sigma_{\text{Sdi}}$ that is imposed by the scaling factor in Equation (4). The right panel of this figure shows that $\zeta_{S_{\text{dtarget}}}$ values computed from Equation (6) are exactly the same as those calculated individually for each alternative ground-motion bin. Therefore, Equation (6) significantly speeds up the computational time, which increases the overall efficiency of the proposed procedure.

3. EXTENDING THE PROPOSED METHODOLOGY FOR NONLINEAR SYSTEMS

The linear relationship established between $\ln(S_{\text{dtarget},\,i}(T))$ and $\varepsilon\sigma_{\text{Sdi}}$ is strictly valid for linear systems and fails when the structure responds in the post-elastic range. This is demonstrated in Figure 3, which shows the relationship between the inelastic spectral displacements ($S_{\text{d},ie}$) and $\varepsilon\sigma_{\text{Sdi}}$ obtained from the scaled recordings of the optimum ground-motion bin discussed in the previous section. The inelastic spectral displacements are computed for strength reduction factors of $R = 2$ (left panel), $R = 4$ (middle panel), and $R = 8$ (right panel) (Elastic strength reduction factor, R, is the ratio of elastic to yield strength of an SDOF system). The solid straight line in each panel shows the target elastic

DOI: 10.1002/eqe

Table I. Fundamental seismological features of the ground-motion dataset and scaling factors of the accelerograms in the optimum recording set for a short-period elastic building of $T_1 = 0.3$ s.

Record name	M_w	R_{JB} (km)	Site[a]	Fault[b]	$S_{d,i}$ (cm)	$\bar{S}_{d,i}$ (cm)	$\varepsilon\sigma_{Sdi}$	γ_i
TGMB1592	**7.1**	**32.1**	**NEHRP D**	**SS**	**0.732**	**0.658**	**0.107**	**2.882**
PEER1794	7.1	31.1	NEHRP C	SS	0.903	0.557	0.483	—
PEER1636	7.4	50.0	NEHRP D	SS	1.046	0.506	0.725	—
PEER1633	7.4	12.6	NEHRP C	SS	2.807	1.223	0.831	—
PEER1144	**7.2**	**43.3**	**NEHRP D**	**SS**	**0.544**	**0.530**	**0.027**	**3.579**
PEER1116	**6.9**	**19.1**	**NEHRP D**	**SS**	**1.042**	**0.945**	**0.098**	**2.007**
PEER1107	6.9	22.5	NEHRP D	SS	1.556	0.823	0.637	—
PEER0880	7.3	27.0	NEHRP D	SS	0.624	0.819	−0.271	—
PEER0864	**7.3**	**11.0**	**NEHRP C**	**SS**	**1.570**	**1.314**	**0.178**	**1.443**
PEER0848	7.3	19.7	NEHRP D	SS	2.467	1.051	0.853	—
PEER0827	7.0	16.0	NEHRP C	R	0.547	1.157	−0.749	—
PEER0826	**7.0**	**40.2**	**NEHRP D**	**R**	**0.837**	**0.637**	**0.272**	**2.975**
PEER0812	**6.9**	**33.9**	**NEHRP C**	**SS**	**0.446**	**0.470**	**−0.053**	**4.031**
PEER0809	**6.9**	**12.2**	**NEHRP C**	**SS**	**1.041**	**1.112**	**−0.066**	**1.704**
PEER0801	**6.9**	**14.2**	**NEHRP C**	**SS**	**0.953**	**0.990**	**−0.038**	**1.914**
PEER0290	6.9	29.8	NEHRP D	N	0.771	0.565	0.310	—
PEER0289	**6.9**	**13.3**	**NEHRP C**	**N**	**0.989**	**0.913**	**0.080**	**2.076**
PEER0288	**6.9**	**22.5**	**NEHRP C**	**N**	**0.704**	**0.594**	**0.169**	**3.190**
PEER0138	7.4	24.1	NEHRP D	R	0.462	1.137	−0.901	—
PEER0015	7.4	38.4	NEHRP C	R	0.864	0.640	0.300	—

[a]NEHRP C and D site classes are classified as 180 m/s ⩽ V_{S30} < 360 m/s and 360 m/s ⩽ V_{S30} < 760 m/s, respectively [23].
[b]SS, N, and R refer to strike–slip, normal, and reverse style-of-faulting, respectively.

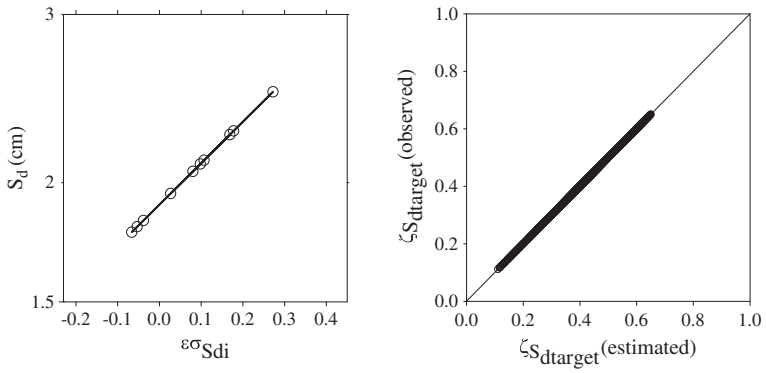

Figure 2. Linear variation of spectral displacement values with respect to $\varepsilon\sigma_{Sdi}$ after scaling (left panel), and estimated versus observed (real) standard deviation values of each alternative ground motion bin (right panel) for an SDOF system of $T = 0.3$ s.

spectral displacement (i.e., $S_{dtarget,i}(T)$) versus $\varepsilon\sigma_{Sdi}$ relationship of the scaled recordings for the elastic response case given in the left panel of Figure 2. The correlation (ρ) between $S_{d,ie}$ and $\varepsilon\sigma_{Sdi}$ is given on the lower right corner of each panel. It decreases significantly with the increasing level of inelasticity (i.e., increasing R). The plots suggest that for a given target hazard level the optimum recording set for a linear structural system is not necessarily the best choice when the same system starts responding beyond its elastic limits.

To select the optimum ground-motion bin for nonlinear response, we modified the proposed method by establishing an empirical relationship between $\varepsilon\sigma_{Sdi}$ and $\varepsilon\sigma_{ISdi}$. The new parameter $\varepsilon\sigma_{ISdi}$ represents the difference between the target hazard level and the inelastic spectra. The level of nonlinearity is represented by strength factor, R. To develop a robust empirical relationship between $\varepsilon\sigma_{Sdi}$ and $\varepsilon\sigma_{ISdi}$, we assembled a ground-motion dataset of 260 accelerograms compiled from the PEER-NGA (http://peer.berkeley.edu) and the Turkish national strong-motion (http://kyh.deprem.gov.tr/ftpe.htm) databases. The accelerograms are selected from NEHRP C and D type soil conditions with a magnitude

DOI: 10.1002/eqe

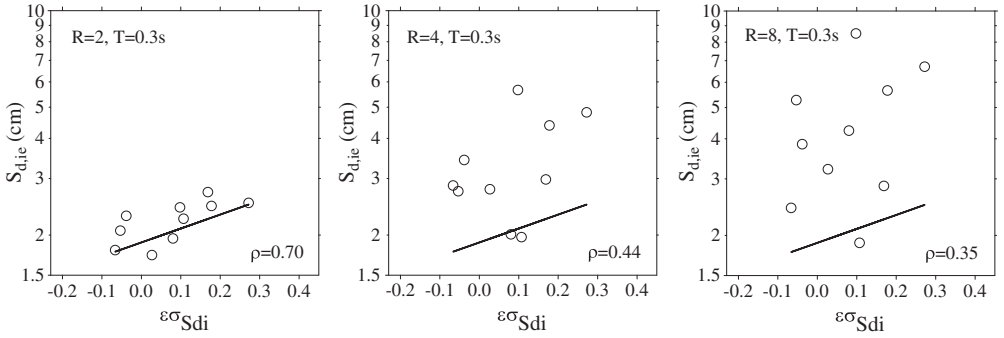

Figure 3. Decreasing correlation between the inelastic spectral displacements of scaled ground motions and $\varepsilon\sigma_{\mathrm{Sdi}}$ with increasing inelasticity level. The black solid lines show the relationship between the target elastic spectral displacement and $\varepsilon\sigma_{\mathrm{Sdi}}$ of the scaled recordings given in Figure 2.

range of $5.0 \leqslant M_w \leqslant 7.7$ and for source-to-site distances (R_{JB}) less than 100 km. The chosen soil conditions are limited to fully understand the effect of soil behavior on ground motion selection and scaling. However, they represent the site classes that are frequently encountered in the urban settlements. The magnitude and source-to-site distance intervals in the dataset are within the common interest range of most engineering projects. Figure 4 shows the magnitude versus source-to-site distance distribution of the selected accelerograms. The vertical and horizontal solid lines on this figure show the magnitude and distance intervals of ground-motion bins that are used for deriving the empirical relationship.

For each bin the target hazard is represented as the central distance and magnitude values. Given a bin we followed the presented scaling procedure and computed $\varepsilon\sigma_{\mathrm{Sdi}}$ values for linear response (Equation (2)) to scale each record to its individual target level, $S_{\mathrm{dtarget},i}(T)$ (Equation (4)). We used the scaled accelerograms to run nonlinear response history analyses for a predetermined set of periods ($T = 0.3$, 0.6, 0.9, 1.2, and 1.5 s) and strength reduction factors ($R = 2$, 4, 6, and 8) to compute the corresponding inelastic spectral displacements. We used a bilinear hysteretic model with a post-yielding stiffness ratio (α) of 3% in nonlinear response history analyses. It is assumed that the chosen hysteretic model can fairly represent the post-elastic behavior of nondegrading RC buildings. Because elastic $\varepsilon\sigma_{\mathrm{Sdi}}$ is defined as the offset between the individual elastic spectral ordinate and θ in logarithmic scale, the inelastic $\varepsilon\sigma_{\mathrm{ISdi}}$ of each recording can be defined as the logarithmic difference between the individual $S_{\mathrm{d},ie}$ and θ. A typical example for the relationship

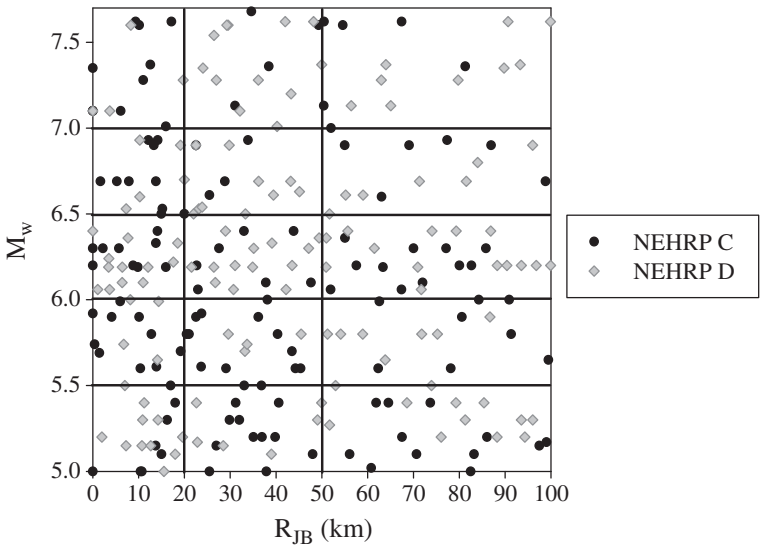

Figure 4. R_{JB} versus M_w scatter in terms of site class and distribution of accelerograms in each ground-motion bin (separated by vertical and horizontal solid lines).

DOI: 10.1002/eqe

between $\varepsilon\sigma_{Sdi}$ and $\varepsilon\sigma_{ISdi}$ is given in Figure 5 for $T=0.6$ s and $R=2$, 4, and 6. Figure 5 depicts that the increase in the inelastic level results in a decrease in the correlation (ρ) between $\varepsilon\sigma_{Sdi}$ and $\varepsilon\sigma_{ISdi}$. Figure 6 gives the overall picture of the entire correlation between these two parameters for all T and R values considered in this study. In addition to the observation made in Figure 5, the correlation plots of this figure indicate a negative influence of shorter periods on the relationship between $\varepsilon\sigma_{Sdi}$ and $\varepsilon\sigma_{ISdi}$ advocating higher dispersion in the nonlinear response of short-period structures.

The above discussions suggest a clear need to improve the correlation between $\varepsilon\sigma_{Sdi}$ and $\varepsilon\sigma_{ISdi}$ for the proposed procedure to rank the alternative ground-motion bins for a certain level of nonlinear response through their dispersion statistics about a target hazard level. To increase the correlation between these parameters, we tested PGV ($\varepsilon\sigma_{PGVi}$) and a linear combination of PGV with a spectral ordinate ($\varepsilon\sigma_{PGVi+Sdi}$) as alternative estimators of $\varepsilon\sigma_{ISdi}$. This idea stems from various recent studies that showed the usefulness of either PGV or combination of PGV with a spectral ordinate while relating nonlinear structural response and selection of strong-motion recordings (e.g. Refs. [27, 28]). The competency and efficiency of $\varepsilon\sigma_{PGVi}$ or $\varepsilon\sigma_{PGVi+Sdi}$ as estimators of $\varepsilon\sigma_{ISdi}$ is given in Figure 7, which presents the correlation between $S_{d,ie}$ versus $\varepsilon\sigma_{PGVi}$ (left panel) and $S_{d,ie}$ versus $\varepsilon\sigma_{PGVi+Sdi}$ (right panel) computed for the case presented previously in Figure 3. Improved correlation between $S_{d,ie}$ versus $\varepsilon\sigma_{PGVi}$ and $S_{d,ie}$ versus $\varepsilon\sigma_{PGVi+Sdi}$ when compared with the correlation given for $\varepsilon\sigma_{Sdi}$ (middle panel in Figure 3) suggests that these new parameters can be used more efficiently in the selection and scaling of recordings for assessing the performance of nonlinear structural systems. Note that the linear combination, $\varepsilon\sigma_{PGVi+Sdi}$, yields a slightly better correlation with inelastic spectral displacement ordinates.

On the basis of these observations, the $\varepsilon\sigma_{ISdi}$ values computed for each bin in the assembled ground-motion dataset is approximated in terms of $\varepsilon\sigma_{PGVi+Sdi}$ through the functional forms given in Equation (7).

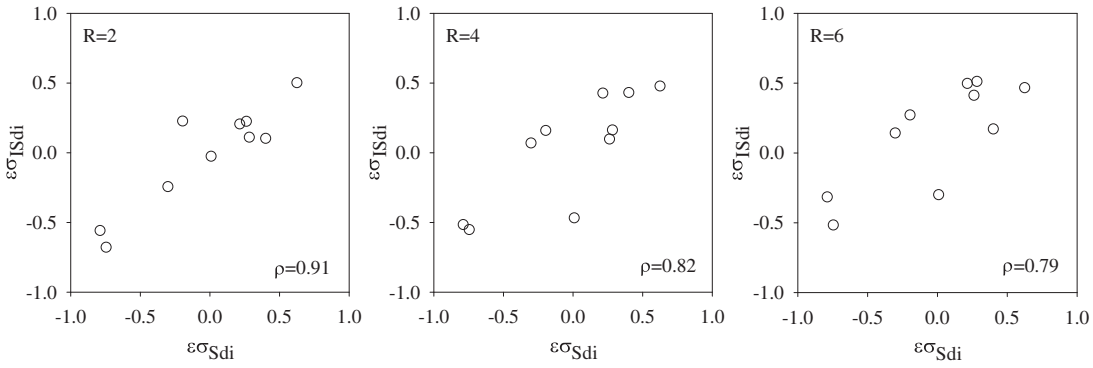

Figure 5. Decreasing correlation between $\varepsilon\sigma_{Sdi}$ and $\varepsilon\sigma_{ISdi}$ values with increasing level of inelasticity for an SDOF system of $T=0.6$ s.

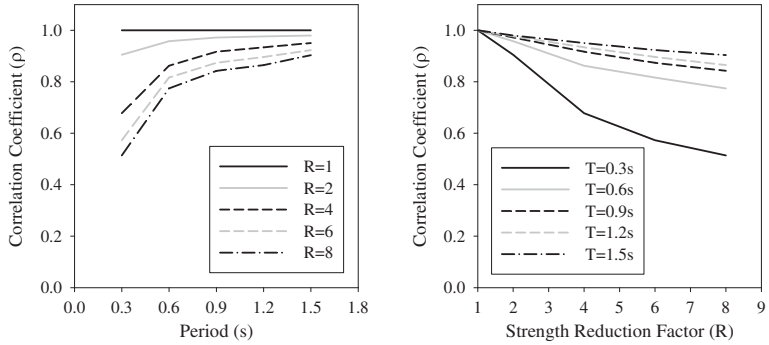

Figure 6. Variation of correlation between $\varepsilon\sigma_{Sdi}$ and $\varepsilon\sigma_{ISdi}$ as a function of T (left panel) and as a function of R (right panel).

DOI: 10.1002/eqe

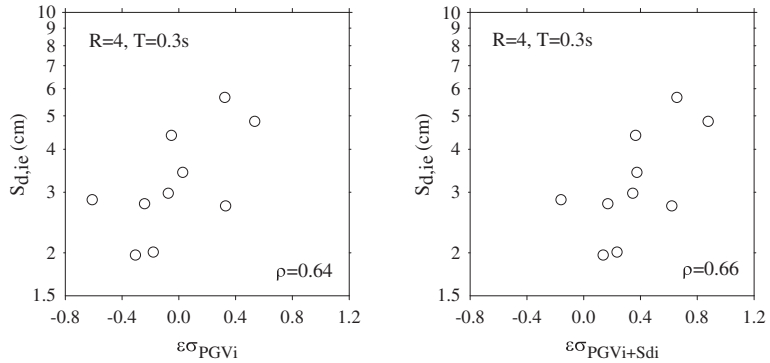

Figure 7. Correlation between inelastic spectral displacements and $\varepsilon\sigma_{\mathrm{PGVi}}$ (left panel) and $\varepsilon\sigma_{\mathrm{PGVi+Sdi}}$ (right panel) for $R=4$ and $T=0.3$ s.

$$\varepsilon\sigma_{\mathrm{ISdi}} = c_1(R,T)\cdot\varepsilon\sigma_{\mathrm{Sdi}} + c_2(R,T)\cdot\varepsilon\sigma_{\mathrm{PGV}} + c_3(R,T) \tag{7.a}$$

$$c_1(R,T) = 1 - 0.72\ln(R) + 0.7T\ln(R) - 0.21T^2\ln(R) \tag{7.b}$$

$$c_2(R,T) = 0.81\ln(R) - 0.78T\ln(R) + 0.23T^2\ln(R) \tag{7.c}$$

$$c_3(R,T) = 0.22\ln(R) - 0.4T\ln(R) + 0.15T^2\ln(R) \tag{7.d}$$

The possible bias in Equation (7) in terms of the seismological parameters magnitude and source-to-site distance (R_{JB} in our study) is investigated by conventional residual analysis. We fit straight lines to the computed residuals that are computed for each T–R pair to observe their likely trends in terms of magnitude and distance (Table II). If the slope term in a straight line is significantly different than zero, Equation (7) can be considered biased for the corresponding seismological parameter. The null hypothesis that the slope term is zero is tested by applying the t-statistics that provide the significance level (p) for rejecting or failing to reject the null hypothesis. A p-value that is above 0.05 is generally accepted as sufficient for failing to reject the null hypothesis; the insignificance of the slope term in the straight line fit. The t-statistics indicate a fairly good performance of Equation (7) as the p-values generally attain values larger than 0.05 for almost all T–R pairs. (See Table II for the list of p-values computed from the residual analysis. Bold p-values show the cases for which the null hypothesis that the slope term of the straight line equals to zero is rejected). This observation suggests an acceptable level of accuracy in the $\varepsilon\sigma_{\mathrm{ISdi}}$ estimates of the proposed model.

The proposed $\varepsilon\sigma_{\mathrm{ISdi}}$ should be used in Equation (6) while ranking the alternative bins populated from a ground-motion dataset of k recordings to identify the optimum bin of recordings while assessing the nonlinear behavior of a structural system. The following section presents a case study to show the limitations and general features of the proposed method by making comparisons with the alternative selecting and scaling methods.

Table II. p-values computed from the residual analysis as a function of M_w and R_{JB}.

p-value		$T=0.3$ s	$T=0.6$ s	$T=0.9$ s	$T=1.2$ s	$T=1.5$ s
M_w	$R=2$	0.477	0.932	0.776	0.729	0.590
	$R=4$	**0.023**	0.807	**0.023**	0.069	0.334
	$R=6$	**0.003**	0.257	0.126	0.317	0.941
	$R=8$	**0.047**	0.593	**0.002**	0.053	0.809
R_{JB}	$R=2$	0.345	0.744	0.115	0.345	**0.036**
	$R=4$	**0.019**	0.175	0.459	0.300	0.858
	$R=6$	0.126	0.160	0.220	0.217	0.230
	$R=8$	0.299	0.333	0.167	0.005	0.053

DOI: 10.1002/eqe

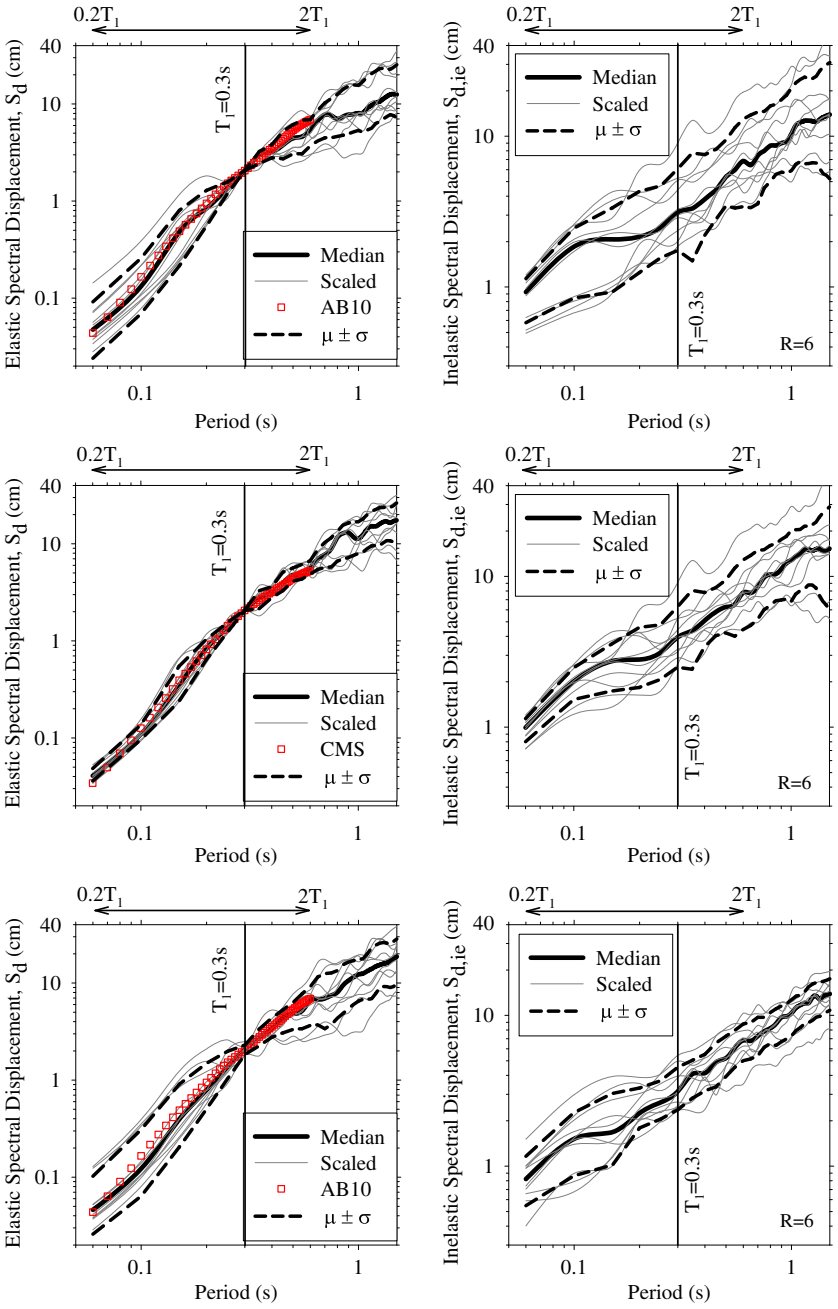

Figure 8. Comparisons of record selection and scaling procedures of Shome *et al.* [4] (1st row), Baker [10] (2nd row) and this study (3rd row) for $T = 0.3$ s. The 1st column plots show the results for linear structural response whereas the panels in the 2nd column give the same information for nonlinear structural response for $R = 6$.

4. CASE STUDY

We compared the proposed methodology with the selection and scaling procedures proposed by Shome *et al.* [4] and Baker [10]. Shome *et al.* [4] emphasized the significance of dispersion (standard deviation) of the selected recordings about the target hazard level. Thus, their proposed methodology scales each individual recording to a common target elastic spectral ordinate that results in zero dispersion about this ground-motion intensity. Although the proponents of this procedure recommend using recordings from magnitude and distance intervals comparable to the

DOI: 10.1002/eqe

Table III. Selected recordings among the candidate accelerograms by the three methods compared in this study.

Record name	This study	CMS, Baker [10]	Shome *et al.* [4]
TGMB1592	—	—	X
PEER1794	—	X	X
PEER1636	X	—	—
PEER1633	—	—	X
PEER1144	X	X	X
PEER1116	—	—	—
PEER1107	X	X	—
PEER0880	—	—	X
PEER0864	X	X	X
PEER0848	X	X	X
PEER0827	X	X	X
PEER0826	—	X	—
PEER0812	—	—	—
PEER0809	—	—	X
PEER0801	X	—	—
PEER0290	—	X	—
PEER0289	X	X	—
PEER0288	X	—	—
PEER0138	—	—	X
PEER0015	X	X	—

target hazard scenario, their conclusive remark is the lesser significance of such restrictions in the implementation of their methodology.

As briefed in Section 1, Baker [10] introduced a new spectral shape, the CMS, for selecting and scaling the strong-motion recordings. In his examples the target scenario is determined from the deaggregation of a site-specific probabilistic seismic hazard analysis (PSHA) that results in a target magnitude (M_{target}) and source-to-site distance (d_{target}) associated with an epsilon value. Baker [10] considered a spectral period band about the fundamental period (T_1) of the structural system such that CMS, as a spectral shape, coincides with the target spectral ordinate at T_1. The CMS spectral ordinates for the rest of the vibration periods are computed by considering the correlation between the epsilon values of each spectral period and the epsilon value at the fundamental period of the structure. The period range of interest is taken as $0.2\,T_1 \leqslant T_1 \leqslant 2.0\,T_1$ in [10]. The CMS method selects and scales the ground motions in two alternative ways. In both cases a ground-motion dataset of k recordings with comparable magnitude and distance ranges to the target scenario are selected. In the first alternative these candidate recordings are scaled to the common target hazard level as in the case of Shome *et al.* [4]. A statistical measure (sum of squared errors, SSE) is set to quantify the match between the response spectrum ordinates of each individual accelerogram and CMS over the period range of interest. The computed SSE values are ranked and the first n recordings with the smallest SSE are selected. In the second alternative each individual accelerogram is scaled such that their average response spectrum and CMS are equal over the period range of interest. The selection among these scaled recordings follows the same statistical criterion used in the first alternative. Baker [10] recommends the use of former alternative because it is simple and performs better with respect to the latter one. Following his recommendation, we implemented his first criterion in the case study.

The comparisons between the methods are made by using the fictitious target scenario given in Section 2 (i.e., $M_w = 7.15$, $R_{\text{JB}} = 22.5$ km and an epsilon value of 1.44 after the deaggregation analysis for $T_1 = 0.3$ s, which results in an elastic target spectral ordinate of 2.06 cm according to the Akkar and Bommer [26] model). The use of a short-period structural system would reveal the limitations of our proposed procedure better because dispersion of inelastic behavior about the target hazard level is significant at shorter vibration periods as discussed in the previous section. While implementing each procedure, we selected 10 recordings ($n = 10$) from a ground-motion dataset of 20 accelerograms ($k = 20$). The ground-motion dataset of candidate accelerograms is already listed in Table I because the fictitious scenario is the same one used in Section 2. The selection of candidate

DOI: 10.1002/eqe

accelerograms that consider the compatibility between the major seismological features of the target scenario and the ground motions is comparable for all procedures. Thus, there is no bias in the identification of candidate accelerograms for the methods verified in this paper.

Figure 8 shows the variation of spectral ordinates for linear and nonlinear structural behavior (mimicked by a bilinear response with $\alpha = 3\%$ and $R = 6$) for the records selected and scaled by the 3 procedures. Table III shows the optimum recordings selected by each procedure. Note that the proposed procedure selects and scales different sets of recordings for linear and nonlinear structural response. Table I has already listed the optimum recordings for the linear case for the proposed procedure and they are not repeated here once again. The spectral ordinates are given for a period band of $0.06\,\text{s} \leqslant T \leqslant 1.5\,\text{s}$, which is wide enough to convey a complete vision about the performance of the methods tested in this study. The first row in Figure 8 shows the record selection and scaling results of the Shome *et al*. [4] method. This is followed by the CMS and our procedure. The left panel in each row shows the performance of investigated methods for the linear response of the chosen structural system. The right panel displays the success of the methods when the system behaves in the post-elastic range for $R = 6$. The plots also show the period-dependent variation of standard deviation of the scaled recordings about their median trends. The linear scaling results of Baker [10] include the hazard-specific CMS that constitutes the basis of the record selection and scaling in his methodology. For the sake of consistency, the left panel plots of Shome *et al*. [4] and this study display the spectral ordinate estimations of Akkar and Bommer [26] for the target hazard scenario.

For linear response, the implementation of the Shome *et al*. [4] and Baker [10] scaling methods results in zero dispersion about the target spectral ordinate at the fundamental period. The corresponding dispersion, although small, is different than zero ($\zeta_{S_{\text{dtarget}}} = 0.111$ as presented in Section 2) in our method because our main purpose is to provide the optimum recording set with reliable information on the associated aleatory variability without suppressing it as in the case of other methods. The median trend of scaled recordings in [10] compares very well with CMS because the selection criterion is directly based on the best match between CMS and individual recordings. Neither the proposed methodology nor that of Shome *et al*. [4] base the record selection criteria on a spectral match over a predetermined period band. Nonetheless, the median elastic spectral ordinates of scaled recordings from these two methods follow the estimations of Akkar and Bommer [26] fairly close for the period range used in [10]. The advantage of CMS emerges in the dispersion statistics because the period-dependent standard deviation of this procedure shows a much smaller variation about the median elastic response of scaled recordings when compared with the other two methods. However, when the nonlinear structural response is of concern, the superior performance of the proposed procedure is indisputable because the dispersion about the median inelastic response of scaled recordings draws a lesser uncertainty with respect to the other methods compared in this study. Moreover, the proposed methodology conveys this

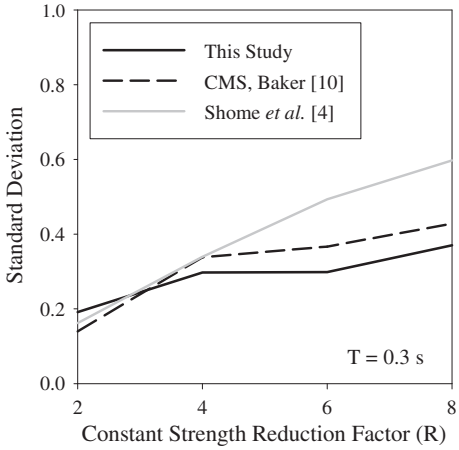

Figure 9. Standard deviation of spectral response obtained by selected and scaled records to the target intensity of the scenario event according to the compared methods.

DOI: 10.1002/eqe

information to the analyst by a proper estimation of the standard deviation at the target hazard level via Equations (6) and (7).

Figure 9 gives a more general view about the performance of the proposed procedure for the record selection and scaling of nonlinear structural response. Using the same fictitious scenario and building, the standard deviations about the median nonlinear response of scaled recordings for different R values are computed for the three methods considered in this section. The comparative curves advocate that the use of the proposed procedure would result in lesser uncertainty for the verification of subject structural system because the selected and scaled recordings of our method yield smaller dispersion about the median nonlinear response for almost all inelastic levels for which the structure can experience during a future scenario earthquake. It is noted that the level of dispersion about the median nonlinear structural response increases with increasing R values regardless of the compared methods; a phenomenon that is discussed in various studies that is also dependent of the structural type (e.g., Refs, [28–30]).

5. SUMMARY AND CONCLUSIONS

We proposed a record selection and scaling procedure that can be used efficiently for the verification of nondegrading nonlinear simple (first-mode dominant) structural systems that are located on soft to stiff soil conditions (referred to as NEHRP D and C site classes, respectively). The procedure selects and scales the ground motions that are compatible with the major seismological features of the target scenario. The selection and scaling is made through a nested layout and each recording is scaled for a specific target intensity level that depends on the spectral ordinate difference between the individual recording and the corresponding estimation from a consistent GMPE. This way, the method prevents the excessive modification of selected ground-motion recordings. The average of scaled ground motions at the period of interest is equal to the target spectral ordinate. The scaled ground motions preserve the aleatory variability inherent in the nature of earthquakes, and the proposed procedure is capable of computing the exact aleatory variability for elastic structural systems. This dispersion can be estimated accurately for structures responding in the nonlinear range. The method in this article defines the optimum recording set as the one that constitutes the minimum dispersion about the target hazard level, which may bring forward the significance of the median structural response. The description of standard deviation of scaled ground motions about the target hazard level would convey important information about the likely distribution of the structural behavior about the median response. This assertion, however, should be tested carefully before the proposed procedure can be recommended as a tool in the probabilistic risk assessment and loss models.

Our comparisons with the selection and scaling procedures of Shome *et al*. [4] and Baker [10] suggest that the proposed methodology can be considered as an efficient tool for the verification of nonlinear structural systems for a given target hazard scenario. The selected and scaled recordings by our procedure result in lesser uncertainty about the median inelastic response with respect to the other two methods. The performance of the method is fairly acceptable for linear structural systems because the median spectral ordinates of the scaled ground motions follow the target hazard level (represented by a predictive model) closely over a wide period range with slightly higher dispersion when compared with the CMS method.

ACKNOWLEDGEMENTS

The authors express their sincere gratitude to two anonymous reviewers who made valuable suggestions to increase the technical quality of the paper.

REFERENCES

1. Nau JM, Hall WJ. Scaling methods for earthquake response spectra. *Journal of Structural Engineering (ASCE)* 1984; **110**(7):1533–1548.
2. Martinez-Rueda JE. Scaling procedure for natural accelerograms based on a system of spectrum intensity scales. *Earthquake Spectra* 1998; **14**(1):135–152.

DOI: 10.1002/eqe

3. Kappos AJ, Kyriakakis P. A re-evaluation of scaling techniques for natural records. *Soil Dynamics and Earthquake Engineering* 2000; **20**:111–123.
4. Shome N, Cornell CA, Bazzurro P, Carballo JE. Earthquakes, records, and nonlinear responses. *Earthquake Spectra* 1998; **14**(3):469–500.
5. Bommer JJ, Acevedo AB. The use of real earthquake accelerograms as input to dynamic analysis. *Journal of Earthquake Engineering* 2004; **8**(Special Issue 1):43–91.
6. Naeim F, Alimoradi A, Pezeshk S. Selection and scaling of ground motion time histories for structural design using genetic algorithms. *Earthquake Spectra* 2004; **20**(2):413–426.
7. Cimellaro GP, Reinhorn AM, D'Ambrisi A, De Stefano M. Fragility analysis and seismic record selection. *Journal of Structural Engineering (ASCE)* 2011; **137**(3):379–390.
8. Watson-Lamprey J, Abrahamson N. Selection of ground motion time series and limits on scaling. *Soil Dynamics and Earthquake Engineering* 2006; **26**:477–482.
9. Luco N, Bazzurro P. Does amplitude scaling of ground motion records result in biased nonlinear structural drift responses? *Earthquake Engineering and Structural Dynamics* 2007; **36**(13):1813–1835.
10. Baker JW. Conditional Mean Spectrum: Tool for ground-motion selection. *Journal of Structural Engineering (ASCE)* 2011; **137**(3):322–331. DOI 10.1061/(ASCE)ST.1943-541X.0000215.
11. Baker JW, Cornell CA. A vector-valued ground motion intensity measure consisting of spectral acceleration and epsilon. *Earthquake Engineering and Structural Dynamics* 2005; **34**(10):1193–1217.
12. Baker JW, Cornell CA. Spectral shape, epsilon and record selection. *Earthquake Engineering and Structural Dynamics* 2006; **35**(9):1077–1095.
13. Haselton CB. Evaluation of ground motion selection and modification methods: Predicting median interstory drift response of buildings. *PEER Report 2009/01*, Pacific Earthquake Engineering Research Center, University of California, Berkeley, 2009.
14. Cordova PP, Deierlein GG, Mehanny SSF, Cornell CA. Development of a two-parameter seismic intensity measure and probabilistic assessment procedure. *The Second U.S.-Japan Workshop on Performance-Based Earthquake Engineering Methodology for Reinforced Concrete Building Structures*, Sapporo, Hokkaido, Japan 2000.
15. International Code Council (ICC). International Building Code. Falls Church, VA, 2006.
16. American Society of Civil Engineers (ASCE). Minimum design loads for buildings and other structures. *ASCE 7–05*. American Society of Civil Engineers/Structural Engineering Institute, Reston, VA, 2005.
17. European Committee for Standardization (CEN). Eurocode 8: Design of structures for earthquake resistance-Part 1: General rules, seismic actions and rules for buildings *EN1998-1*. Brussels, 2004.
18. Reyes JC, Kalkan E. How many records should be used in ASCE/SEI-7 ground motion scaling procedure. *Earthquake Spectra* 2011; (in-press).
19. Hancock J, Bommer JJ, Stafford PJ. Numbers of scaled and matched accelerograms required for inelastic dynamic analyses. *Earthquake Engineering and Structural Dynamics* 2008; **37**(14):1585–1607.
20. TEC. Specification for buildings to be built in seismic zones. *TEC-07*, Ministry of Public Works and Settlement, Government of Republic of Turkey, Ankara, Turkey, 2007.
21. Applied Technology Council, ATC-58. Guidelines for seismic performance assessment of buildings. *ATC-58 50% Draft*, Redwood City, CA, 2009.
22. Stewart JP, Chiou SJ, Bray JD, Graves RW, Somerville PG, Abrahamson NA. Ground motion evaluation procedures for performance-based design. *PEER Report 2001/09*, Pacific Earthquake Engineering Research Center, University of California, Berkeley, 2001.
23. Building Seismic Safety Council (BSSC). NEHRP recommended provisions for seismic regulations for new buildings and other structures. *FEMA P-750*, Washington, DC, 2009.
24. The MathWorks Inc. MATLAB Version 7.11. Natick, MA, USA, 2011.
25. Buratti N, Stafford PJ, Bommer JJ. Earthquake accelerogram selection and scaling procedures for estimating the distribution of drift response. *Journal of Structural Engineering (ASCE)* 2011; **137**(3):345–357. DOI 10.1061/(ASCE)ST.1943-541X.0000217.
26. Akkar S, Bommer JJ. Empirical equations for the prediction of PGA, PGV, and spectral accelerations in Europe, the Mediterranean Region, and the Middle East. *Seismological Research Letters* 2010; **81**(2):195–206
27. Mousavi M, Ghafory-Ashtiany M, Azarbakht A. A new indicator of elastic spectral shape for the reliable selection of ground motion records. *Earthquake Engineering and Structural Dynamics* 2011; **40**(7). DOI 10.1002/eqe.1096.
28. Akkar S, Özen Ö. Effect of peak ground velocity on deformation demands for SDOF systems. *Earthquake Engineering and Structural Dynamics* 2005; **34**(13):1551–1571.
29. Ruiz-Garcia J, Miranda E. Inelastic displacement ratios for evaluation of existing structures. *Earthquake Engineering and Structural Dynamics* 2003; **32**(8):1237–1258. DOI 10.1002/eqe.271.
30. Akkar S, Küçükdoğan B. Direct use of PGV for estimating peak nonlinear oscillator displacements. *Earthquake Engineering and Structural Dynamics* 2008; **37**(12):1411–1433.